



Molecular Crystals and Liquid Crystals

Publication details, including instructions for authors and subscription information:

<http://www.tandfonline.com/loi/gmcl20>

Effect of an External Field on the Director Profile of a Nematic Liquid Crystal Around a Spherical Particle

Jun-ichi Fukuda^{a b} & Hiroshi Yokoyama^{a b}

^a Nanotechnology Research Institute (NRI), National Institute of Advanced Industrial Science and Technology (AIST), Umezono, Tsukuba, Japan

^b Liquid Crystal Nano-System Project, ERATO/SORST, Japan Science and Technology Agency, Tokodai, Tsukuba, Japan

Version of record first published: 22 Sep 2010

To cite this article: Jun-ichi Fukuda & Hiroshi Yokoyama (2007): Effect of an External Field on the Director Profile of a Nematic Liquid Crystal Around a Spherical Particle, *Molecular Crystals and Liquid Crystals*, 475:1, 165-172

To link to this article: <http://dx.doi.org/10.1080/15421400701675366>

PLEASE SCROLL DOWN FOR ARTICLE

Full terms and conditions of use: <http://www.tandfonline.com/page/terms-and-conditions>

This article may be used for research, teaching, and private study purposes. Any substantial or systematic reproduction, redistribution, reselling, loan, sub-licensing, systematic supply, or distribution in any form to anyone is expressly forbidden.

The publisher does not give any warranty express or implied or make any representation that the contents will be complete or accurate or up to date. The accuracy of any instructions, formulae, and drug doses should be independently verified with primary sources. The publisher shall not be liable for any loss, actions, claims, proceedings, demand, or costs or damages whatsoever or howsoever caused arising directly or indirectly in connection with or arising out of the use of this material.

Effect of an External Field on the Director Profile of a Nematic Liquid Crystal Around a Spherical Particle

Jun-ichi Fukuda
Hiroshi Yokoyama

Nanotechnology Research Institute (NRI), National Institute of Advanced Industrial Science and Technology (AIST), Umezono, Tsukuba, Japan; Liquid Crystal Nano-System Project, ERATO/SORST, Japan Science and Technology Agency, Tokodai, Tsukuba, Japan

In our previous study we have demonstrated that an adaptive mesh refinement scheme can be effectively used to investigate the orientation profiles of a nematic liquid crystal around a spherical particle when the characteristic size of the defect core is much smaller than the particle radius. We have also shown that the dynamics of a nematic liquid crystal can be properly treated to reproduce the experimentally observed structural transition from the hedgehog to the Saturn ring configuration induced by an external field. As a preliminary study for the quantitative investigation of this transition, we study in this article how the choice of the criterion for mesh refinement/unrefinement influences the stability of the hedgehog under an external field in our numerical system. The severer is the criterion for mesh refinement to produce a larger number of fine grids, the weaker field can induce the transition. Nevertheless, the dependence of the critical field strength on the criterion for mesh refinement is weak and the criterion can be systematically controlled. Therefore our numerical scheme is shown to be safely applied to the quantitative study on the stability of the hedgehog configuration under an external field.

Keywords: adaptive mesh; colloid; external field; hyperbolic hedgehog; nematic liquid crystal; Saturn ring

I. INTRODUCTION

As a novel class of composite materials containing liquid crystals (LCs), LC colloid dispersions have attracted much interest in

We thank Dr. Philippe Poulin, conversation with whom motivated this work.

Address correspondence to Jun-ichi Fukuda, Nanotechnology Research Institute, AIST, 1-1-1 Umezono, Tsukuba 305-8568, Japan. E-mail: fukuda.jun-ichi@aist.go.jp

technology as well as in fundamental science [1,2]. One of the fascinating aspects of LC colloidal dispersions from the fundamental viewpoint is that due to the anchoring at the surfaces of colloidal particles, the surrounding LCs show elastic distortions, which, in the cases of strong surface anchoring, result in topological defects accompanying the colloidal particles.

When a spherical particle with homeotropic surface anchoring is immersed in a uniformly aligned nematic LC, two types of topological defects accompanying a particle are possible and indeed observed experimentally; a point-like hyperbolic hedgehog [1,3] and a ring-like defect referred to as a Saturn ring [4,5]. Which one is stable depends on various factors including the strength of the surface anchoring and the particle radius [2,6]. For large particles (whose radius is larger than about $1\text{ }\mu\text{m}$) with sufficiently strong surface anchoring, a hyperbolic hedgehog is energetically preferred [2,6].

Concerning those two configurations, it was predicted [6] and verified experimentally [7] that a hedgehog becomes unstable to transform into a Saturn ring when an external electric or magnetic field is applied parallel to the far-field nematic director. In our previous numerical studies using adaptive mesh refinement scheme [8], we have reproduced the dynamics of this transition successfully. However, what determines the threshold field strength to induce the transition still remains unclear. Together with his numerical results, Stark [6,9] gives a discussion on the field strength H_1 under which the hedgehog and Saturn-ring configurations have equal free energies. But his theoretical argument is based on a rough estimate of the volume of the highly distorted region in those two configurations, and a precise estimate of H_1 is absent. Moreover, due to the possible large energy barrier between those two configurations, it is unlikely that the transition occurs at H_1 ; presumably the hedgehog configuration must become absolutely unstable for the transition to take place. There have been, however, almost no analytic or numerical attempts to estimate this critical field strength H_2 under which a hyperbolic hedgehog accompanying a spherical particle becomes unstable. Although Stark gives a numerical estimate of H_2 for one given particle radius [6], how the critical field H_2 depends on the important factors such as the particle radius is yet to be understood.

In this article we present the results of our preliminary study for a systematic investigation of the critical field strength H_2 . Our final goal is to find the dependence of H_2 on the particle radius in the case of rigid normal surface anchoring. We use an adaptive mesh refinement scheme developed previously [10,11] in order to overcome the numerical difficulty arising from the coexistence of two largely different

characteristic lengths: the size of the defect core (of the order of 10 nm) and the particle radius ($\gtrsim \mu\text{m}$). Although we have succeeded in demonstrating the dynamics of the transition from a hedgehog to a Saturn ring under an external field [8], one has to take care when the critical field strength H_2 is to be determined numerically; the numerical H_2 may be dependent on how the numerical grids are prepared. We also notice that even when one uses regular grids without adaptive mesh refinement, the numerical H_2 may depend on the resolution of the grids; in the extreme case, “numerical pinning” can occur in very coarse grids [6]. In this article we investigate how the numerical H_2 may depend on the criterion for mesh refinement/unrefinement. We show that the severer criterion for mesh refinement is employed so that a larger number of fine grids are generated, the weaker the numerical H_2 is. But the dependence of the numerical H_2 on the criterion is weak, and we also discuss how the criterion can be systematically controlled. Therefore, when the criterion for the mesh refinement is appropriately chosen, our numerical scheme is reliable for the investigation of the critical field strength H_2 for the stability of a hyperbolic hedgehog.

This article is organized as follows: in Section II we present the model for numerical calculations of the orientational order profile and its dynamics. We present our numerical results in Section III. We conclude this article in Section IV.

II. MODEL

Here we present only the essential points of our numerical calculations and detailed description of our numerical scheme is given in Refs. [8,11]. We employ a second-rank symmetric and traceless tensor order parameter Q_{ij} instead of a director n for the description of the orientational order of a nematic LC. We write the free energy density in the bulk as $f = f_{LdG}(Q_{ij}) + f_{el}(Q_{ij}, \nabla) + f_{ext}(Q_{ij}, \tilde{\mathbf{H}})$. Here $f_{LdG}(Q_{ij})$ is the local energy density in terms of the Landau-de Gennes expansion. It reads

$$f_{LdG} = -\frac{1}{2}A\text{Tr}Q^2 - \frac{1}{3}B\text{Tr}Q^3 + \frac{1}{4}C(\text{Tr}Q^2)^2, \quad (1)$$

where $\text{Tr}Q^2 = Q_{ij}Q_{ij}$ and $\text{Tr}Q^3 = Q_{ij}Q_{jk}Q_{ki}$ (summation over repeated indices is implied). For positive A , B and C , a uniaxial configuration $Q_{ij} = Q_{bulk}(n_i n_j - (1/3)\delta_{ij})$ with positive Q_{bulk} minimizes f_{LdG} . The f_{el} is the elastic energy due to the inhomogeneous LC orientation. We adopt the following simple one-constant form:

$$f_{el} = \frac{1}{2}L_1 \partial_k Q_{ij} \partial_k Q_{ij}, \quad (2)$$

where L_1 is the elastic constant. We employ the free energy density due to the (dimensionless) external field $\tilde{\mathbf{H}}$ that reads

$$f_{ext} = -\tilde{\mathbf{H}}_i \tilde{\mathbf{H}}_j \frac{Q_{ij}}{\sqrt{\text{Tr} \mathbf{Q}^2}} \quad (3)$$

The minus sign in front of the right-hand-side of eq. (3) indicates that the director tends to be parallel to the field. The reason for not choosing the usual form $-\tilde{\mathbf{H}}_i \tilde{\mathbf{H}}_j Q_{ij}$ is given in detail in Ref. [8]. We briefly mention here that under this choice the strength of the nematic ordering Q_{bulk} is independent of the field strength and the director, which conforms to the fixed boundary conditions given below. This treatment is justified for a deep nematic state that is considered throughout this study.

As in the previous study [8], we choose $C = B = 3A$ and then $Q_{bulk} = 1$ minimizes f_{LdG} . With this choice, the dimensionless field $\tilde{\mathbf{H}}$ is associated with the dimensional one \mathbf{H} as $\tilde{\mathbf{H}}^2 = \Delta\chi H^2 / \sqrt{6}$, where $\Delta\chi$ is the anisotropy of the susceptibility. We set the direction of $\tilde{\mathbf{H}}$ along the z -axis and therefore $\tilde{\mathbf{H}} = \tilde{H} \delta_{iz}$.

As the boundary conditions, we assume rigid normal anchoring at the particle surface and set $Q_{ij}(r = R_0) = Q_{bulk}(e_i^r e_j^r - (1/3)\delta_{ij})$, where R_0 is the particle radius, r is the distance from the center of the particle, and e^r is a unit vector along the radial direction. We impose uniform alignment along the z -axis (or the field direction) at infinity by setting $Q_{ij}(r = \infty) = Q_{bulk}(e_i^z e_j^z - (1/3)\delta_{ij}) = Q_{bulk}(\delta_{iz}\delta_{jz} - (1/3)\delta_{ij})$. This setup corresponds to placing one spherical particle of radius R_0 with rigid normal anchoring in a nematic LC uniformly aligned along the z -axis. We also note that since the particle surface gives a Dirichlet boundary condition, the corresponding surface free energy does not appear in the total free energy of the system.

As the equation for describing the dynamics of the order parameter Q_{ij} , we employ the following simple relaxation equation:

$$\frac{\partial}{\partial t} Q_{ij}(\mathbf{r}) = -\Gamma \frac{\partial F}{\partial Q_{ij}(\mathbf{r})} + \lambda \delta_{ij}, \quad (4)$$

where $F = f_{|r|>R_0}(f_{LdG} + f_{el} + f_{ext})$ is the total free energy of the system and Γ is a kinetic coefficient associated with rotational viscosity. The Lagrange multiplier λ ensures $\text{Tr} \mathbf{Q} = Q_{ii} = 0$.

To construct our numerical system, we introduce a variable $\zeta = R_0^{-1} - r^{-1}$. We assume rotational symmetry about the z -axis and prepare initial 33×65 grids in the (ζ, θ) space with $0 \leq \zeta \leq R_0^{-1}$ (corresponding to $R_0 \leq r \leq \infty$), and $0 \leq \theta \leq \pi$ (θ is the polar angle measured from the z -axis). From the initial grids, we allow mesh refinement by bisections up to eight levels and our numerical system

corresponds to $(2^{13} + 1) \times (2^{14} + 1)$ non-adaptive grids. We monitor the spatial variation at every given numerical steps and if the index at a given numerical cell

$$\epsilon = (\partial_k Q_{ij} \partial_{kj} Q_{ij})^2 r^2 \Delta \zeta \Delta \theta \simeq (\partial_k Q_{ij} \partial_k Q_{ij})^2 \times \frac{\Delta S}{r} \quad (5)$$

exceeds some criterial value ϵ_f , the cell is refined by bisection, and if the sum of ϵ 's at four cell is smaller than another criterial value ϵ_c , the four cells are united to a coarser one. Here $\Delta S \simeq \Delta r (r \Delta \theta) \simeq r^3 \Delta \zeta \Delta \theta$ is the size of the cell in (two-dimensional) real space.

The size of the defect core is characterized by the nematic correlation length $\xi = \sqrt{L_1/A}$. Therefore it is natural to choose $C\xi$, with C being some small numerical factor, as the finest grid spacings in real space, i.e., Δr and $r \Delta \theta$. Since $r \simeq R_0$ and $\partial_k Q_{ij} \partial_k Q_{ij} \simeq (A/L_1)$ around the defect core, ϵ_f and ϵ_c should be proportional to $A/(L_1 R_0)$. In the following, we present our numerical results concerning the criterion for mesh rearrangement in terms of $\tilde{\epsilon}_f \equiv \epsilon_f L_1 R_0 / A$. We always choose $\epsilon_c = 0.25 \epsilon_f$.

III. RESULTS

Before presenting our numerical results, we introduce some dimensionless variables characterizing the system: the dimensionless particle radius $\bar{R}_0 \equiv R_0/\xi = R_0/\sqrt{L_1/A}$, and the (further-rescaled) field strength $h \equiv \bar{H}/\sqrt{A}$. We notice that the field strength has been rescaled so that h remains unchanged when R_0 is varied.

Figure 1 shows the orientation profiles of a nematic LC around a spherical particle and the corresponding numerical grids for different $\tilde{\epsilon}_f$'s. The field strength h is chosen just below the critical field strength h_2 , so that the hedgehog configuration is metastable, but not unstable. The distorted regions indicated by gray and white regions are localized near the particle surface due to the external field, and the width of the distorted region is essentially determined by the correlation length associated with the external field. The grid profiles shown in Figures 1(c) and (d) clearly indicate that smaller $\tilde{\epsilon}_f$ forces a larger number of fine grids to be generated. But still, $\tilde{\epsilon}_f = 4 \times 10^{-3}$ is sufficient for the description of the static structure of the hedgehog defect core much smaller than the particle size. From Figure 1 one can also find that the hedgehog defect is made up of a small ring, not a point, as already shown in our previous study [11].

In Figure 2, we plot the dependence of the critical field strength h_2 for the stability of the hedgehog configuration on the criterial parameter $\tilde{\epsilon}_f$ for mesh rearrangement for three different particle radii

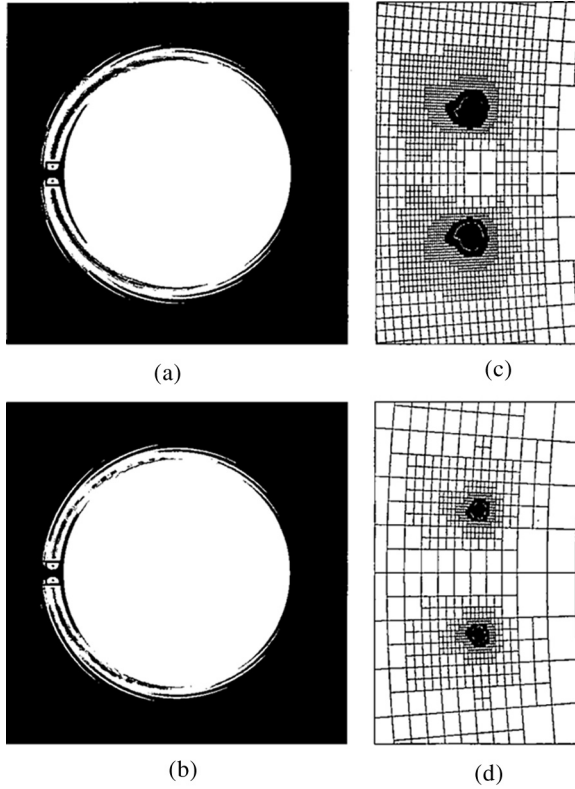


FIGURE 1 Orientation profiles are shown in (a) and (b) as gray-scale plots of Q_{zz}^2 for $\bar{R}_0 = 274$ (z -direction is the horizontal direction and in the black region the director is along the z -direction). Parameters are (a) $\tilde{\epsilon}_f = 8 \times 10^{-4}$ and $h = 3.42 \times 10^{-2}$ and (b) $\tilde{\epsilon}_f = 4 \times 10^{-3}$ and $h = 3.85 \times 10^{-2}$. Those field strengths are just below h_2 . (c) and (d) represent the numerical grids for (a) and (b), respectively, in the clipped regions indicated by rectangles in (a) and (b). The regions (c) and (d) are of the same size.

\bar{R}_0 's. Preparation of a larger number of fine grids can reduce the possible effect of numerical pinning. Therefore, as we can readily expect, weaker field can induce the structural transition when $\tilde{\epsilon}_f$ is reduced and a larger number of fine grids are generated. But the dependence of h_2 on $\tilde{\epsilon}_f$ is weak and systematic; the qualitative behavior of h_2 with the variation of the particle radius \bar{R}_0 remains the same for different and fixed $\tilde{\epsilon}_f$'s. From this result we can conclude that when the criterion for mesh rearrangement is appropriately and systematically chosen, our adaptive mesh refinement scheme can be safely used for a

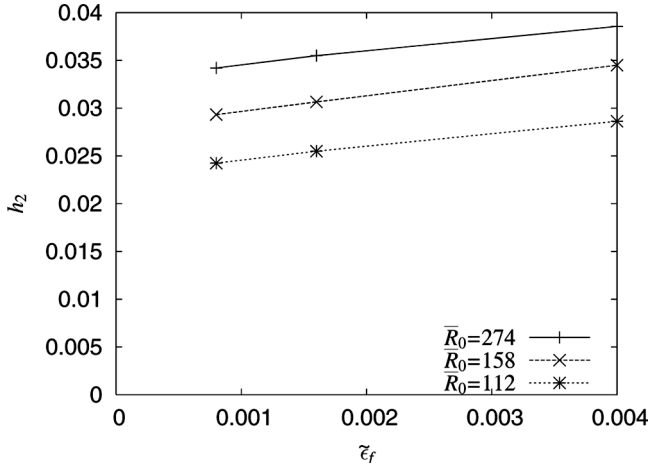


FIGURE 2 Dependence of the rescaled critical field strength h_2 for the stability of the hedgehog configuration on the criterion parameter $\tilde{\epsilon}_f$ for mesh rearrangement. Data are shown for three different particle radii \bar{R}_0 's.

quantitative as well as qualitative investigation on the stability of a hedgehog accompanying a spherical particle under an applied external field.

IV. CONCLUSION

In this article we have presented our preliminary study on the stability of a hyperbolic hedgehog accompanying a spherical particle in a uniformly aligned nematic liquid crystal under an applied external field. We have focused on the validity of our previously developed numerical scheme based on an adaptive mesh refinement, in particular how the choice of the criterion for mesh rearrangement influences the numerical behavior of a hyperbolic hedgehog. We have shown that when the criterion parameter $\tilde{\epsilon}_f$ for mesh rearrangement is varied, the critical field strength h_2 for the stability of a hedgehog also changes. But the dependence of h_2 on $\tilde{\epsilon}_f$ is weak enough and systematic in that the behavior of h_2 with the variation of the particle radius \bar{R}_0 is the same for different and fixed $\tilde{\epsilon}_f$'s. Therefore under a systematic control of the criterion for mesh rearrangement, our numerical scheme using adaptive mesh refinement can be safely used for investigating quantitatively as well as qualitatively the stability of the hedgehog configuration under an applied external field. In future publication we will present our extensive and systematic studies on

the stability of the hedgehog configuration together with the energetics of the hedgehog and the Saturn ring configurations and discuss which factor determines the stability of the hedgehog configuration and how the critical field strength depends on the particle radius.

REFERENCES

- [1] Poulin, P., Stark, H., Lubensky, T. C., & Weitz, D. A. (1997). *Science*, 275, 1770.
- [2] Stark, H. (2001). *Phys. Rep.*, 351, 387.
- [3] Poulin, P. & Weitz, D. A. (1998). *Phys. Rev. E*, 57, 626.
- [4] Mondain-Monval, O., Dedieu, J. C., Gulik-Krzywicki, T., & Poulin, P. (1999). *Eur. Phys. J. B*, 12, 167.
- [5] Gu, Y. & Abbott, N. L. (2000). *Phys. Rev. Lett.*, 85, 4719.
- [6] Stark, H. (1999). *Eur. Phys. J. B*, 10, 311.
- [7] Loudet, J. C. & Poulin, P. (2001). *Phys. Rev. Lett.*, 87, 165503.
- [8] Fukuda, J., Yoneya, M., & Yokoyama, H. (2004). *Mol. Cryst. Liq. Cryst.*, 413, 221;
Fukuda, J., Stark, H., Yoneya, M., & Yokoyama, H. (2004). *J. Phys.: Condens. Matter*, 16, S1957.
- [9] Stark, H. (2002). *Phys. Rev. E*, 66, 032701.
- [10] Fukuda, J. & Yokoyama, H. (2001). *Eur. Phys. J. E*, 4, 389.
- [11] Fukuda, J., Yoneya, M., & Yokoyama, H. (2004). *Phys. Rev. E*, 65, 041709; (2002) *Eur. Phys. J. E*, 13, 87.